

Controlled Synthesis of Monodispersed Cerium Oxide Nanoparticle Sols Applicable to Preparing Ordered Self-Assemblies

Noriya Izu,* Ichiro Matsubara, Toshio Itoh, Woosuck Shin, and Maiko Nishibori

National Institute of Advanced Industrial Science and Technology (AIST), Advanced Manufacturing Research Institute, 2266-98 Anagahora, Shimo-Shidami, Moriyama-ku, Nagoya 463-8560

Received October 23, 2007; E-mail: n-izu@aist.go.jp

Highly dispersed metal oxide nanoparticle sols are of great interest in science and engineering because of their broad potential applications in optics, electronics, sensors, catalysis, biomedicines, and even in cosmetics. Here, we report the size-controlled synthesis of cerium oxide nanoparticle sols by a reflux method with poly(vinylpyrrolidone) as a coating agent to afford stable monodispersions of spherical particles with size of 50–120 nm. The size of nanoparticles can be easily controlled by appropriate adjustment of the molecular weight of the added polymer. Colloidal crystals of cerium oxide are also obtained by evaporation of the cerium oxide sol. As cerium oxide has a larger refractive index than silica and polymers typically used for the preparation of colloidal crystals, the present sols are expected to be useful for the fabrication of high-performance photonic crystals.

Dispersions (sols) of metal oxide nanoparticles are of interest in various scientific and technological fields. For example, sols of dielectric nanoparticles are used to make dielectric devices,[1] sols of silica nanoparticles are used to make colloidal crystals,[2,3] sols of MFe_2O_4 (M = Fe, Co, and Mn) have been used in the production of magnetic nanodevices and biomedicines,[4] and sols of cerium oxide nanoparticles are used for chemical mechanical polishing (CMP).[5–8] Cerium oxide itself exhibits a range of useful functions, including high oxygen storage capacity,[9–13] high diffusion coefficient for the oxide ion,[14,15] high refractive index,[16,17] and high ultraviolet (UV) absorption,[5,18] and is used in a range of applications; as a promoter in three-way catalysts,[9–13] in resistive oxygen gas sensors,[19–23] in photonic crystals,[24] and in oxide ion conductors.[25–27] A number of devices incorporating cerium oxide are now in practical use. The sol of cerium oxide nanoparticles is used not only in CMP but also as a UV absorbent.[5–8,18] Nanoparticles of cerium oxide have been the focus of substantial research, and it has been revealed in a number of studies that the nanoparticles are spherical, with a particle size of 50–500 nm and a narrow size distribution.[28–32] However, there appear to be no reports on the preparation of stable sols of such cerium oxide nanoparticles, which would be useful for the synthesis of high-performance colloidal crystals (i.e., photonic crystals) in addition to the applications above. Although there are some commercialized sols including cerium oxide nanoparticles, the shape of the nanoparticles in the sols are not spherical but polyhedral. The dispersion of nanoparticles in a medium can be improved by applying a process that prevents particle aggregation simultaneously with the synthesis of particles, as breaking down the aggregation after synthesis is difficult. Aggregation prevention is usually performed by coating the surface of the nanoparticles with a polymer. Recently, a reflux method has been reported[28] as a method for precipitating cerium oxide nanoparticles, although the addition of alkaline substances is the common method.[5,33]

In this study, a sol of cerium oxide spherical nanoparticles is prepared by a reflux method whose synthesis conditions are much different from Ref. 28, and the dispersion of the sol is investigated. By optimizing the synthesis conditions using cerium nitrate as the source material and poly(vinylpyrrolidone) (PVP) as the polymer, a sol of PVP-coated cerium oxide nanoparticles is obtained with good dispersion of spherical particles of 50–120 nm in size with a narrow size distribution. The size of nanoparticles can be controlled by appropriate adjustment of the molecular weight of the polymer added during synthesis. The method proposed here for the control of nanoparticle size is novel, and contrasts with the conventional method of changing the concentration of the source material. Ordered self-aggregations can be prepared using the sol, with possible applications in the fabrication of photonic crystals.

Experimental

As-Prepared Dispersion Sol and Dried Powder. Poly(vinylpyrrolidone) (PVP; Sigma-Aldrich or Acros) and cerium nitrate $Ce(NO_3)_3 \cdot 6H_2O$ (Kojundo Chemical Laboratory) were added to 30 cm^3 of ethylene glycol (Wako Pure Chemical Industries) and stirred. The concentrations of PVP and cerium nitrate in the solution were 120 kg m^{-3} and 0.600 kmol m^{-3}, respectively. PVP additives with average molecular weights of 4350–18000 were tested. Molecular weights were determined by gel permeation chromatography calibrated against poly(ethylene glycol). The mixture was heated under reflux to the boiling point of ethylene glycol (190 °C) for 15–20 min, yielding a white sol. A powder of the as-prepared sol was prepared by removal of unreacted material and excess PVP by centrifugation (10000–18000 rpm), followed by washing with water and ethanol and drying at 80 °C.

Redispersed Sol. Redispersion was investigated by dispersing the dried nanoparticle powder in a range of media (water, ethanol, terpineol, and ethylene glycol). The ratio of powder to dispersion medium was fixed at 0.1 g per 5 cm^3 in all cases. After mixing the powder into the dispersion medium, the mixture was homogenized

Published on the web June 11, 2008; doi:10.1246/bcsj.81.761

by ultrasonication (30 W) for 3–10 min under cooling but without dispersing agents to afford a redispersed sol.

Assemblies. The redispersed sols were heated to 50 or 60 °C for slow evaporation of ethanol to afford fibrous and crystalloid nanoparticle assemblies. Assemblies were also prepared by rapid evaporation in a heated oven at 80 °C.

Characterization. The obtained nanoparticles, sols, and assemblies were characterized by X-ray diffraction (XRD) analysis, scanning electron microscopy (SEM), transmission electron microscopy (TEM), Fourier transform infrared (FTIR) spectroscopy, thermogravimetry (TG), dynamic light scattering (DLS) measurements, viscosity measurements, ultraviolet (UV)–visible spectroscopy, and optical microscopy. XRD analysis was carried out using a RINT 2100V/PC instrument (Rigaku Corporation) equipped with a copper source (Cu Kα). SEM was carried out using a JSM-6335FM microscope (JEOL Ltd.) equipped with a field-emission gun. TEM was carried out using a JEM-2010 instrument (JEOL Ltd.). FTIR spectroscopy was carried out using an FT/IR-610 spectrometer (JASCO Corporation). TG was carried out using a TGD7000RH-S instrument (ULVAC Sniku-Riko) at a heating rate of 15 °C min^{-1}. DLS was performed using an FPAR-1000I instrument (Otsuka Electronics Co., Ltd.), and the particle size was estimated using the software provided. UV–visible spectroscopy was carried using an MSV-370 microspectrophotometer (JASCO Corporation) with a sampling area of 100 μm × 100 μm and incidence angle of 67°.

Results and Discussion

Characterization of Nanoparticle Powder. A dry powder of the as-prepared sol was used for characterization of nanoparticles. A cerium oxide sol prepared with a reflux time of 15 min using PVP with a molecular weight of 4350 was centrifuged and washed with water and ethanol to remove unreacted materials and excess PVP. The resultant product was then dried at 80 °C to eliminate the dispersion medium to afford a dry powder.

The X-ray diffraction (XRD) pattern of the powder displays diffraction peaks identical to that given by card 34-0934 of the Joint Committee on Powder Diffraction Standards (JCPDS), confirming that the powder is cerium oxide (Figure 1). The crystallite size determined from the full-width at half-maximum of the diffraction peaks on the Williamson–Hall plot is approximately 3 nm. Figure 2a shows a scanning electron microscopy (SEM) image of the nanoparticle powder, revealing spherical particles with uniform size. The average particle size determined from the SEM images is 114 nm with a coefficient of variation of 0.120 (standard deviation divided by average). Figure 2b shows a transmission electron microscopy (TEM) image of one of the 110 nm particles. The gray rim and black core of the particle suggest that the particles observed are aggregates of much smaller crystallite particles with size of approximately 3 nm.

When ammonium cerium(IV) nitrate $(NH_4)_2Ce(NO_3)_6$ was used instead of cerium nitrate in the synthesis process, the obtained nanoparticles were not CeO_2 but $Ce(HCOO)_3$. The morphology of the particles was not spherical but rod, and the sol of the nanoparticles showed poor dispersion. When the PVP concentration was changed from 120 to 16 kg m^{-3}, the obtained sol of the nanoparticles showed poor dispersion. When the PVP concentration was changed from 120 to 160 kg m^{-3}, no nanoparticles were obtained. These results imply that an optimum concentration of PVP exists to obtain a high dispersion sol. The experimental conditions to obtain a high dispersion sol of cerium oxide nanoparticles were much different from that of Ref. 28.

Thermogravimetry (TG) analysis revealed a gradual weight loss of 5% with heating to 150 °C and a sudden weight loss of 15% with further heating to 300 °C (Figure 3). Heating the powder to 900 °C resulted in a total weight loss of 21%. These results indicate that the powder is composed of not only cerium oxide but also other materials that are decomposed by heat-

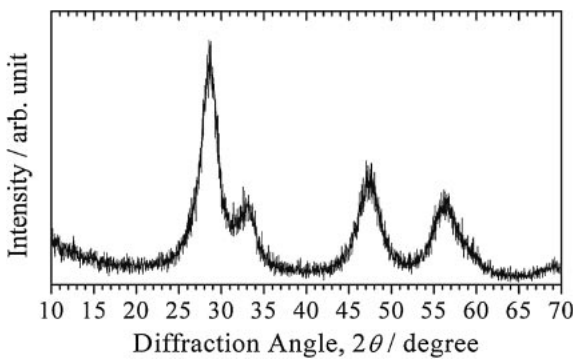

Figure 1. XRD pattern of nanoparticle powder (dry powder of as-prepared sol) prepared under the following conditions: PVP molecular weight of 4350 and reflux time of 15 min.

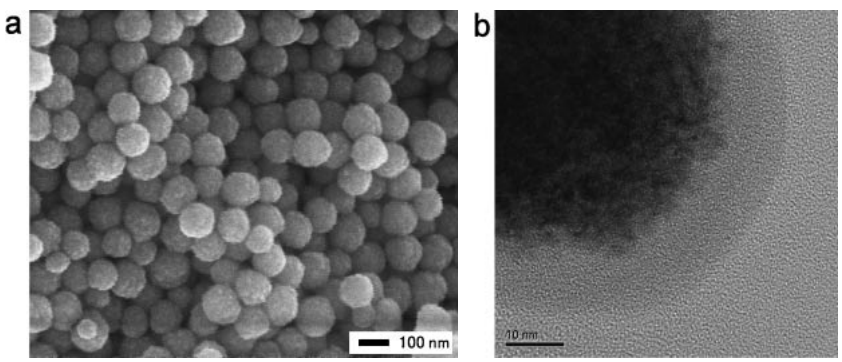

Figure 2. Microstructure of nanoparticle powder prepared under the following conditions: PVP molecular weight of 4350 and reflux time of 15 min: (a) SEM image; (b) TEM image.

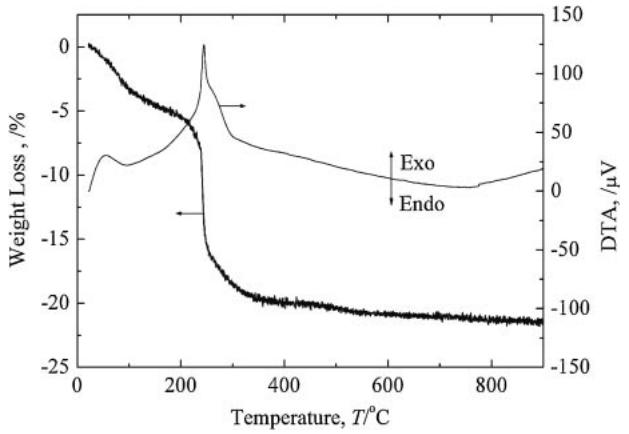

Figure 3. TG curve of nanoparticle powder (dry powder of as-prepared sol) prepared under the following conditions: PVP molecular weight of 4350 and reflux time of 15 min.

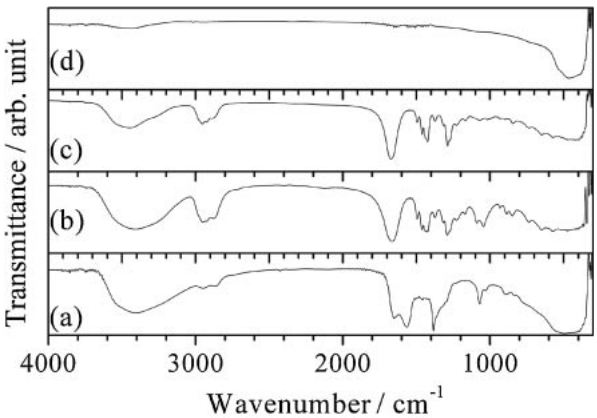

Figure 4. FTIR spectra of various powders: (a) nanoparticle powder (dry powder of as-prepared sol) prepared under the following conditions: PVP molecular weight of 4350 and reflux time of 15 min, (b) dried powder of the sample obtained after a reflux experiment of PVP + EG without $Ce(NO_3)_3 \cdot 6H_2O$ at 190 °C, (c) PVP powder, (d) commercial CeO_2 powder (Mitsuwa Chemicals Co., Ltd.).

ing. This is confirmed by Fourier transform infrared (FTIR) spectrum (Figure 4), which contains peaks not attributable to cerium oxide. The unknown peaks are thought to be attributable to the rim layer on particles observed by TEM. The FTIR spectrum for the rim layer is similar to that of PVP (Figure 4), which would have decomposed under exposure to the electron beam during TEM observations. These results suggest that that polymer was absorbed on the surface of the secondary particles of cerium oxide.

We demonstrated the reflux method using hydroxypropyl cellulose with a molecular weight of 15000–30000 (HPC, Wako Pure Chemical Industries) instead of PVP. Other experimental conditions were the same as those described in the Experimental Section. The experimental results using HPC were almost the same as those using PVP. The XRD pattern of the obtained particles showed cerium oxide. The particle shape was spherical. The average particle size determined from the SEM images was 90 nm with a coefficient of variation of 0.22. These results suggested that not only PVP but also other

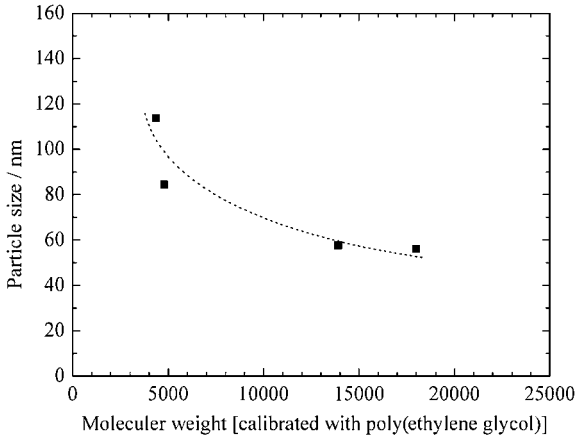

Figure 5. Average size of nanoparticles obtained by synthesis using PVP with a molecular weight of 4350, 4790, 13900, or 18000.

polymers are applicable to the reflux method presented in this study.

Control of Particle Size. Reflux experiments were carried out using a range of molecular weights of PVP (4350, 4790, 13900, and 18000) to determine the effect on particle size. The average size of nanoparticles obtained in these experiments is shown in Figure 5. The average particle size decreased with increasing molecular weight of PVP. The coefficient of variation for all samples was 15% or less, indicating monodispersal of particles in all cases. The particle size of the as-prepared dispersion sols, as determined by dynamic light scattering (DLS) measurements, is consistent with that of the powder determined from SEM images. Therefore, the size of nanoparticles appears to be controllable by appropriate adjustment of the molecular weight of the polymer added to prevent aggregation.

We discuss the control of the particle size by the adjustment of the molecular weight of PVP. If the molecular weight of PVP becomes larger in a solution, a larger force is needed for the migration of PVP. This macroscopic phenomenon is the increase of viscosity of the liquid. For example, the viscosity increases with increasing molecular weight of PVP added into a liquid, when the weight of PVP added is constant. The formation mechanism of nanoparticles is considered to be that primary particles of cerium oxide nucleate and aggregate to grow secondary particles. Because the space of the nucleation is several nanometers,[34] PVP has to be excluded in order to increase the size of the secondary particles to tens of nanometers. Although a small force is needed for the exclusion of PVP of low molecular weight, a larger force is needed in the case of high molecular weight. In the case of high molecular weight, it is considered that the growth rate of the secondary particles is small owing to the large force, and the growth stops early because of the formation of PVP layer around the secondary particles. This may be the reason why the particle size decreases with increasing molecular weight of PVP. In the future, we will clarify the details of the formation mechanism by analysis of the polymer layer on the surface of the nanoparticles.

Recently, a size control method in hydrothermal synthesis of cerium oxide nanoparticles has been reported, in which the size of cerium oxide nanoparticles is controlled by the molar ratio of PVP to cerium nitrate and the concentration of ce-

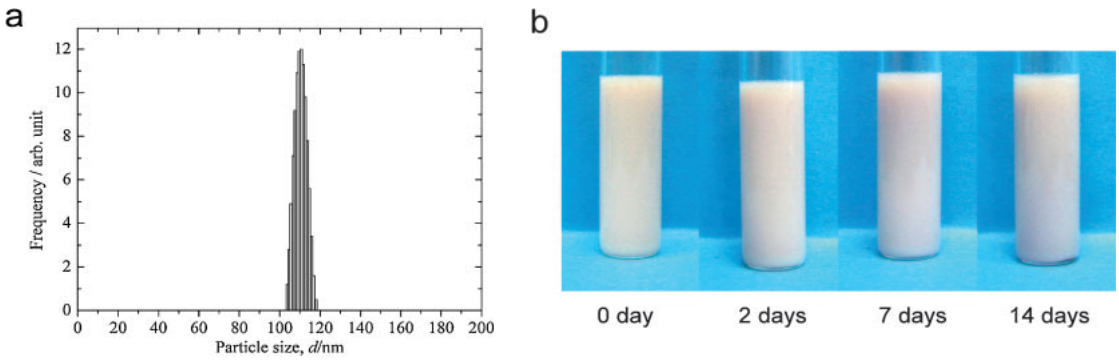

Figure 6. As-prepared sol and redispersed sol of cerium oxide nanoparticles: (a) Size distribution of nanoparticles in as-prepared sol; (b) Photographs of redispersed sol in ethylene glycol (depth: 4 cm).

Table 1. Parameters of Redispersed Sols of Cerium Oxide Nanoparticles

Dispersion medium	After redispersion				Appearance after 7 days
	1 day		8 days		
	Particle size/nm	CV[a)]	Particle size/nm	CV[a)]	
Water	121	0.172	121	0.138	16% transparent layer
Ethanol	115	0.261	117	0.273	13% transparent layer
Terpineol	120	0.131	129	0.133	No change
Ethylene glycol	101	0.221	104	0.135	No change

a) Coefficient of variation.

rium nitrate.[35] In the report, the size is controlled by not molecular weight but molar ratio. Therefore, the reported method is much different from our result. The control of particle size by adjustment of molecular weight of PVP may be useful for improvement of monodispersity of the nanoparticles, because the molecular weight distribution of PVP used in this study is not monodispersive but polydispersive. If the molecular weight distribution becomes narrow, we would obtain more monodispersed cerium oxide nanoparticles. The improvement of monodispersity is difficult by the particle size control method described in Ref. 35. Therefore, it is considered that controlling particle size using the molecular weight of PVP is superior to that described in Ref. 35.

Characterization of Sols. The size distribution of nanoparticles in the as-prepared dispersion sol is shown in Figure 6a. The average particle size is 110 nm, with a coefficient of variation of 0.065, consistent with the results obtained by SEM observations. This result demonstrates that the spherical particles are completely separated in ethylene glycol. This good dispersion may be due to coating with PVP. It is considered that aggregation is prevented by coating with PVP because the polymer is lyophilic in dispersion media, and/or that the polymer coating acts as a barrier to aggregation.

The DLS particle size of the sols prepared by redispersing the dried powder in various media is shown in Table 1. The results show that dispersion was very good even in the case of redispersion. The size of cerium oxide nanoparticles in the redispersed sol after 1 day is approximately equal to that after 8 days, indicating that aggregation did not occur even after 7–8 days. Figure 6b shows photographs of a redispersed sol of cerium oxide nanoparticles in ethylene glycol after 0, 2, 7, and 14 days. No precipitation or transparent layer was observed in these samples, demonstrating that the redispersed sols are stable over extended periods. Redispersion in water or ethanol resulted in the appearance of a transparent layer on the surface of the sol after 7 days, indicating that sedimentation of the nanoparticles occurred. The transparent layer was not observed in the case of redispersion in terpineol or ethylene glycol. The transparent layer appears due to the ready sedimentation in water and ethanol, which have lower viscosity (ca. 1 mPa s)[36,37] compared to terpineol or ethylene glycol (10–40 mPa s).[38,39] After 4 months, the redispersed terpineol and ethylene glycol sols exhibited approximately only 10% of transparent layer at the top of the sols, while approximately 90% of the sol was transparent in the case of the water and ethanol sols. This further demonstrates the stability of the terpineol and ethylene glycol sols. However, the opaque layer in all cases was still soft, and uniform dispersion could be achieved with small vibration. The ability for redispersion is attributed to the PVP coating on the cerium oxide nanoparticles.

Characterization of Nanoparticle Assembly. Assemblies of nanoparticles were obtained by slow and rapid evaporation of ethanol from the sols by heating at different temperatures. Figure 7a shows an optical micrograph of the resultant assemblies obtained by slow evaporation. The formation of assemblies of silica has been reported to occur through the formation of homogeneous films followed by the generation and propagation of cracks and the formation of fibers.[40] The formation mechanism of the assembly prepared by slow evaporation appears to be similar to that of silica.[40] Cracks in the lower layers of the assembly could be observed through the upper layers in the optical micrographs, indicating that this assembly transmit-

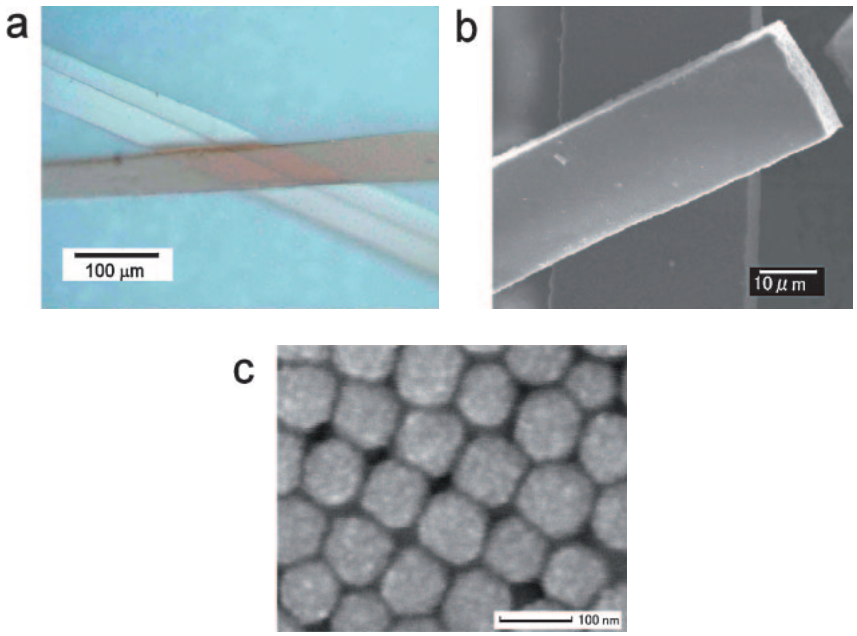

Figure 7. Microstructure of assemblies formed by slow evaporation: (a) Optical micrograph; (b) SEM image; (c) High-magnification SEM image.

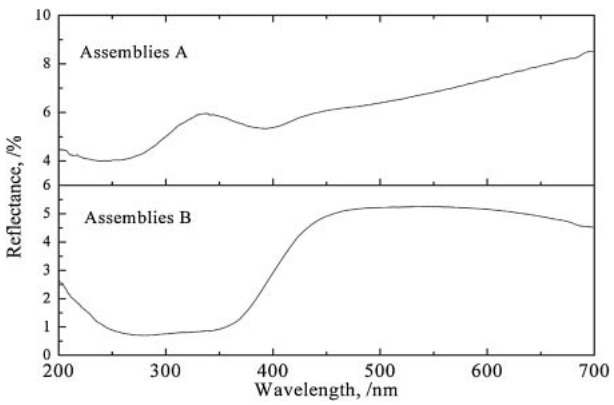

Figure 8. UV–visible spectra for assemblies formed by slow (A) and rapid (B) evaporation.

ted visible light. The SEM image of the assembly (Figure 7b) reveals a structure of rectangular parallelepipeds with very smooth planes. The ordered structure as shown in Figure 7c was observed on the surface of the assembly, although not whole.

Figure 8 shows the ultraviolet (UV)–visible reflectance spectra of both assemblies. In the case of the assembly prepared by rapid evaporation, the reflectance is constant over a wavelength range of 250 to 350 nm, above which the reflectance increases with wavelength from 350 to 450 nm. The slow-evaporation assembly, on the other hand, exhibits a peak reflectance near 330 nm. The wavelength (λ) of light reflected by Bragg diffraction owing to the ordered arrangement of nanoparticles can be calculated by the following equation:[2,41]

$$\lambda = 2D(n^2_{\text{eff}} - \sin^2\theta)^{0.5}, \quad (1)$$

where

$$n^2_{\text{eff}} = n^2{}_1V_1 + n^2{}_2V_2. \quad (2)$$

Here, D is the spacing between planes, n_{eff} is the average refractive index, θ is the angle between the incident ray and scattering planes, n_i is the refractive index of component i, and V_i is the volume of component i. As the average size of nanoparticles is 110 nm, D is 110 nm. The value of θ of the UV–visible instrument is 67°. If the structure of the arrangement of nanoparticles is assumed to be face-centered cubic (fcc), $V_1 = 0.74$ and $V_2 = 0.26$. Using values of $n_1 = 2.1$[16,17] and $n_2 = 1$, the calculated wavelength of reflected light is $\lambda = 359$ nm, which is only 10% larger than the experimental value. The difference between the calculated and experimental values may be due to the influence of the PVP coating on the nanoparticles, as the PVP layer cannot be included in these calculations. The reflectance peak at 330 nm is thus attributed to the ordered arrangement of nanoparticles, representing a colloidal crystal (i.e., photonic crystal). This result therefore indicates that the nanoparticles underwent ordered self-arrangement during evaporation. In general, if the particles have no spherical structure or small size distribution, an assembly with ordered structure can not be obtained. Therefore, the realization of ordered self-arrangement is evidence that the nanoparticles have spherical shape with narrow size distribution. The broadness of the peak suggests the inclusion of many defects in the assembly. Nevertheless, it is expected that a highly ordered structure can be obtained through optimization of the synthesis process of assembly and the preparation of a sol containing spherical particles with a very narrow size distribution.

Conclusion

By a very simple synthesis process, sols of polymer-coated spherical and monodispersed cerium oxide nanoparticles were obtained. Coating the nanoparticles with a lyophilic polymer (PVP) was found to be effective for promoting good dispersion in a range of media. Self-assembled structures of nanoparticles were obtained easily by evaporation of the sols, and the or-

dered arrangement of nanoparticles in the resultant assemblies was found to be excellent. As there are many applications of cerium oxide nanoparticles in dry and sol form, the present results represent a valuable contribution to progress in the science and technology of cerium oxide nanoparticles. In future research, we plan to make spherical nanoparticles of cerium oxide with a very narrow size distribution and a colloidal crystal with more highly ordered structure.

We thank Y. Hayakawa for helpful discussions on gel permeation chromatography, E. Watanabe for centrifuge processing, and T. Kimura for helpful discussions on TEM.

References

1 W. Zhang, L. Xue, X. Zhou, D. Sun, S. Yin, *J. Eur. Ceram. Soc.* **2006**, *26*, 2793.
2 A. S. Sinitskii, A. V. Knot'ko, Y. D. Tretyakov, *Solid State Ionics* **2004**, *172*, 477.
3 P. Jiang, G. N. Ostojic, R. Narat, D. M. Mittleman, V. L. Colvin, *Adv. Mater.* **2001**, *13*, 389.
4 S. Sun, H. Zeng, D. B. Robinson, S. Raoux, P. M. Rice, S. X. Wang, G. Li, *J. Am. Chem. Soc.* **2004**, *126*, 273.
5 J.-S. Lee, J.-S. Lee, S. C. Choi, *Mater. Lett.* **2005**, *59*, 395.
6 T. Sato, T. Katakura, S. Yin, T. Fujimoto, S. Yabe, *Solid State Ionics* **2004**, *172*, 377.
7 D. S. Lim, J. W. Ahn, H. S. Park, J. H. Shin, *Surf. Coat. Technol.* **2005**, *200*, 1751.
8 J.-P. Hsu, A. Nacu, *J. Colloid Interface Sci.* **2004**, *274*, 277.
9 H. C. Yao, Y. F. Yu Yao, *J. Catal.* **1984**, *86*, 254.
10 T. Miki, T. Ogawa, M. Haneda, N. Kakuta, A. Ueno, S. Tateishi, S. Matsuura, M. Sato, *J. Phys. Chem.* **1990**, *94*, 6464.
11 M. Ozawa, M. Kimura, A. Isogai, *J. Mater. Sci.* **1991**, *26*, 4818.
12 M. Ozawa, *J. Alloys Compd.* **1998**, *275–277*, 886.
13 A. Trovarelli, C. de Leitenburg, G. Dolcetti, *CHEMTECH* **1997**, *27*, 32.
14 F. Millot, P. De Mierry, *J. Phys. Chem. Solids* **1985**, *46*, 797.
15 M. Kamiya, E. Shimada, Y. Ikuma, M. Komatsu, H. Haneda, *J. Electrochem. Soc.* **2000**, *147*, 1222.
16 M. Mogensen, N. M. Sammes, G. A. Tompsett, *Solid State Ionics* **2000**, *129*, 63.
17 T. Masui, K. Fukuhara, N. Imanaka, T. Sakata, H. Mori, G. Adachi, *Chem. Lett.* **2002**, 474.
18 R. Li, S. Yabe, M. Yamashita, S. Momose, S. Yoshida, S. Yin, T. Sato, *Solid State Ionics* **2002**, *151*, 235.
19 H.-J. Beie, A. Gnörich, *Sens. Actuators, B* **1991**, *4*, 393.
20 J. Gerblinger, W. Lohwasser, U. Lampe, H. Meixner, *Sens. Actuators, B* **1995**, *26*, 93.
21 G. Sberveglieri, *Sens. Actuators, B* **1995**, *23*, 103.
22 N. Izu, W. Shin, I. Matsubara, N. Murayama, *Sens. Actuators, B* **2004**, *100*, 411.
23 N. Izu, W. Shin, I. Matsubara, N. Murayama, *J. Electroceram.* **2004**, *13*, 703.
24 I. Rodriguez, P. Atienzar, F. Ramiro-Manzano, F. Meseguer, A. Corma, H. Garcia, *Photonics Nanostruct. Fundam. Appl.* **2005**, *3*, 148.
25 K. Huang, M. Feng, J. B. Goodenough, *J. Am. Ceram. Soc.* **1998**, *81*, 357.
26 N. M. Sammes, Z. Cai, *Solid State Ionics* **1997**, *100*, 39.
27 J. A. Kilner, R. J. Brook, *Solid State Ionics* **1982**, *6*, 237.
28 C. Ho, J. C. Yu, T. Kwong, A. C. Mak, S. Lai, *Chem. Mater.* **2005**, *17*, 4514.
29 W. P. Hsu, L. Rönnquist, E. Matijević, *Langmuir* **1988**, *4*, 31.
30 X. Chu, W. Chung, L. D. Schmidt, *J. Am. Cerm. Soc.* **1993**, *76*, 2115.
31 B. Aiken, W. P. Hsu, E. Matijević, *J. Am. Ceram. Soc.* **1988**, *71*, 845.
32 E. Matijević, W. P. Hsu, *J. Colloid Interface Sci.* **1987**, *118*, 506.
33 S. Boskovic, D. Djurovic, Z. Dohcevic-Mitrovic, Z. Popovic, M. Zinkevich, F. Aldinger, *J. Power Sources* **2005**, *145*, 237.
34 T. Ashida, K. Miura, T. Nomoto, S. Yagi, H. Sumida, G. Kutluk, K. Soda, H. Namatame, M. Taniguchi, *Surf. Sci.* **2007**, *601*, 3898.
35 F. Zhou, X. Zhao, H. Xu, C. Yuan, *J. Phys. Chem. C* **2007**, *111*, 1651.
36 M. Ramírez-Gilly, L. P. Martínez-Padilla, O. Manero, *J. Food Eng.* **2007**, *78*, 1117.
37 Y. Zhu, Q. Yang, H. Zheng, L. Gao, Z. Yang, Y. Qian, *Mater. Chem. Phys.* **2006**, *96*, 506.
38 B. Kim, Y. H. Lee, J.-H. Ryu, K.-D. Suh, *Colloids Surf., A* **2006**, *273*, 161.
39 H. Tavana, A. W. Neumann, *Colloids Surf., A* **2006**, *282–283*, 256.
40 H. Nakamura, A. Shimizu, Y. Suyama, *J. Ceram. Soc. Jpn.* **2001**, *109*, 83.
41 G. Mertens, T. Röder, R. Schweines, K. Huber, H.-S. Kitzerow, *Appl. Phys. Lett.* **2002**, *80*, 1885.